A98-31493 ICAS-98-R,2,1

AEROTHERMODYNAMIC CHARACTERISTICS OF TWO-DIMENSIONAL BLUFF BODIES IN HYPERSONIC VISCOUS FLOWS

V. V. Riabov*
Daniel Webster College, Nashua, New Hampshire, 03063-1300, USA
and
I. V. Yegorov† and M. V. Yegorova‡
Central Aero-Hydrodynamics Institute (TsAGI), Zhukovsky-3, Moscow region, Russia 140160

Abstract

The flow structure about two-dimensional bluff bodies (two irregular cylinders in tandem, plate-cylinder configurations, and torus) in hypersonic viscous flow has been studied. The grid equations approximated the Navier-Stokes equations were numerically solved by application of the second-order implicit monotonized scheme, the modified Newton's method, and the Christoffel-Schwarz grid-transformation technique. In transitional rarefied-gas-flow regime, the results are obtained by the direct simulation Monte Carlo technique. The strong influence of the geometrical factors of interference between a plate and a cylinder, and between two cylinders on skin friction and heat flux along the body surfaces has been found. The Reynolds analogy between these parameters does not take place. The drag coefficient of the second cylinder changes non-monotonously with increasing the Reynolds number. The flow parameters in subsonic recirculation zones between the bodies have been analyzed in detail. A new type of shock-wave interference has been found in hypersonic flow near a torus. The drag coefficient, the location of the stagnation points on the torus surface, pressure and skin-friction are sensitive to the inner-to-outer-radii ratio. The study indicates a complex structure of hypersonic flows near bluff bodies and nonlinear effects in distributions of aerothermodynamic parameters.

Nomenclature

C_f = local skin friction coefficient
C_p = local pressure coefficient
C_x = drag coefficient
H = distance between theaxis of symmetry and the torus disk center
$Kn_{\infty R}$ = Knudsen number
L = length of the plate
M = Mach number
p = pressure
q_w = heat flux at the surface
R = radius of a torus disk
$Re_{\infty r}$ = Reynolds number
r = radius of the cylinder
T = temperature
γ = specific heat ratio
Δ = distance between the bodies

Introduction

Numerical and experimental studies[1-5] of simple-shape-body aerothermodynamics have provided valuable information related to physics of hypersonic flows about spacecraft elements and testing devices. Numerous results had been found in the cases of plates, wedges, cones, disks, spheres, and cylinders (see Refs. 1-8).

In the present study, the hypersonic viscous flow about a binary group of the bodies (plate-circular cylinder, two irregular cylinders) and torus has been studied. The effect of body interference is specifically analyzed. The cases considered would be appropriate models of measurement devices, tools for controlling separation and recirculation zones fuel-combustion techniques, and, after certain modification, they can be used in simulating hypersonic viscous flows about segmented projectiles[9].

The structures of hypersonic viscous flow near a sharp flat plate and a cylinder were studied in detail by many researches (i.e., see Refs. 1-6). Koppenwallner[1], Oguchi[2], Allegre and Bisch[3], and others showed that the local skin friction coefficient, the surface pressure, and temperature are maximal near the leading edge of the plate. In a strong interaction hypersonic-flow regime, the influence of the skin friction drag on the total drag can be estimated as 80-90%.[7] Bisch offered a unique experimental technique[7] of the friction reduction by adding a wire-shaped "fore-leading edge" in front of the plate. The experiments of Coudeville et al[5] were helpful for the analysis of the wakes behind cylinders in hypersonic rarefied gas flow.

The structures of incompressible viscous flow between the cylinders in tandem and after different bluff bodies were studied in detail by many researches (i.e., see a review of Blevins[10]). It was found that drag on downstream cylinder was very sensitive to the distance between the cylinders. Δ.

*Adjunct Associate Professor, Dept. of Engineering, Math. & Science, 20 University Drive. Member AIAA.
†Leading Scientist, Aerothermodynamics Division.
‡Research Scientist, Aerothermodynamics Division.

21st ICAS Congress
13-18 September 1998
Melbourne, Australia

and it even changed sign at $\Delta/r < 2$. The case of compressible viscous flow between the cylinders has not been discussed yet.

In the present analysis, the major regularities in hypersonic viscous flow about plate-cylinder configurations and two irregular cylinders in tandem have been studied. The analysis of two-dimensional flow structure is based on numerical solutions of the Navier-Stokes equations using an implicit monotonized scheme of second-order accuracy (Total Variation Diminishing scheme) and Newton's method for solving the grid equations.[11,12] The influence of the Reynolds number and the geometrical factor of interference between the bodies, Δ/r, on skin-friction, heat flux, and pressure in the flow field and along the surfaces of the cylinders has been studied.

Hypersonic rarefied-gas flows near a torus can be a good model in simulating inlet flows in engines, fuel pipes, probes, and pressure tubes. The flow pattern has not been yet discussed in research literature. Several specific features of the flow are unique. For example, if the distance between the axis of symmetry and the torus disk center, H, is significantly larger the torus radius R, ($H \gg R$), than the flow can be approximated by a stream between two side-by-side cylinders[10]. At $H = R$, the flow can be simulated by a stream about a bluff disk.

In the first case, two conical shock waves would focus and interact in the vicinity of the symmetry axis generating the Mach-disk shock wave and the conical reflected waves. The stagnation points would be near the front points of the torus disks. In the second case, the front shock wave would be normal and the location of stagnation points would be difficult to predict. At $H > R$, the flow pattern and shock-wave shapes are very complex. As a result, simple approximation techniques would not be applied in torus aerothermodynamics.

In the present study, flow structure about a torus and its aerodynamic characteristics have been studied under the conditions of hypersonic rarefied-gas flows at $8R \geqslant H \geqslant 2R$ and the Knudsen number $Kn_{\infty R}$ from 0.0167 to 1. The numerical results have been received by the direct simulation Monte Carlo (DSMC) technique[13]. The DS2G computer code was developed by Graeme Bird.[14]

Navier-Stokes Equations and Boundary Conditions.

The unsteady two-dimensional Navier-Stokes equations in a curvilinear coordinate system have been described in Refs. 9, 11, 12, and 15. The no-slip conditions, extrapolations of pressure from inner area nodes and constant surface temperature were posed on the body surface. On the outer surface of the computational area around the body, boundary conditions were written in the form of Riemann invariants and determined by the direction of perturbation expansion.[15]

The Equations Approximation and Numerical Method

The construction of a finite-difference scheme to solve the Navier-Stokes equations given in conservation-law forms is based upon an integro-interpolation method.[15] The scheme is implicit, and this property of the scheme allows to avoid any restrictions on the iteration time-step caused by the instability of the regular difference schemes in the solution of the stiff differential equations.

At semi-integer nodes, the convective components of the flux vectors were approximated using a monotonized scheme of the Godunov's type.[16] The eigenvalues and eigenvectors at the nodes were calculated by the Roe's method[17]. It allows to satisfy the "entropy criterion" in the choosing of a numerical solution with the correct physical properties. To increase the order of finite-difference approximations up to the second one, the Monotone-Upstream-Scheme-for-Conservation-Laws principle of the minimum derivatives[18] was used to interpolate dependent variables on the node side. The diffusion components of the flux vectors at the node side were approximated by the second order central difference scheme.

The difference scheme pattern used for the approximation of the Navier-Stokes equations consists of 13 nodes. The developed implicit nonlinear finite-difference scheme is absolutely stable in the case of the linear problem. The computational mesh was made by numerical solution of the Christoffel-Schwarz transformation problem.[19] The technique of the mesh adaptation in the boundary layers at high Reynolds numbers[20] has been used in this study. The nonlinear system of grid equations was solved using the modified Newton's iteration method.[11,15]

In order to reduce the total number of the arithmetic operations and economize on RAM, the variables were numbered using the generalized method of nested dissection.[21] This technique was successfully used many times in computational experiments and proved its effectiveness and reliability.[15]

Calculations were carried out at the Work Station RS6000/58H. In the case of cylinder-plate configurations, the calculations were performed on the 101×101 grid of the O-type and the computing time of each variant was estimated as approximately 20 min. The calculations of the flow between two irregular cylinders in-tandem were performed on the 101×151 grid of the H-type. The computing time of each variant was estimated as approximately 3h. 20 min.

DSMC Method

The DSMC method has been used in this study as a numerical simulation technique for low-density hypersonic gas flows. The basic principles of the technique were described by Bird[13]. The axisymmetrical DSMC code[14] is used in this study. Molecular collisions in argon are modeled using the variable hard sphere (VHS) molecular model[13]. The gas-surface interactions are assumed to be fully diffusive with full moment and energy accommodation. The code validation was tested by the author[8] in comparing numerical results with experimental data[4,8] related to the simple-shape bodies.

Numerical Results

Cylinder-Plate Configuration

The flowfield around the circular cylinder of radius r and a plate of length $L = 2r$ was calculated for the Mach number $M_\infty = 5$ and the Reynolds number $Re_{\infty r} = 10^4$ and 10^5. It was assumed that $\gamma = 1.4$, and the body surface is isothermal at $T_w/T_\infty = 2$. The four cases were studied: 1) the cylinder alone without a plate; 2) the distance between the leading edge of the plate and the rear point of the cylinder is $\Delta/r = 0$; 3) $\Delta/r = 1$; 4) $\Delta/r = 2$.

The contours of constant values of local Mach number M at $Re_{\infty r} = 10^5$ are shown in Fig. 1. Under the testing conditions, the flow can be characterized by existing shock waves near the cylinder and in the wakes behind it, as well as by a wide separation area in the rear zone of the cylinder. The main differences of the flow patterns occur in this zone.

The distributions of flow parameters along the plane of symmetry in the wakes behind the cylinder at $Re_{\infty r} = 10^5$ are shown in Fig. 2. The geometrical factor of plate location, Δ/r, influences significantly the Mach number parameters. The pressure profiles are the same in the cases considered.

The existence of the plate changes significantly the parameters of the flow near the rear part of the cylinder at $Re_{\infty r} = 10^4$ (see Fig. 3). The heat flux on the rear cylindrical surface is extremely sensitive to the plate location. At $\Delta/r = 0$, the heat flux decreases by the factor of 10 in comparison with the case of flow around the cylinder without a plate. But at $\Delta/r = 2$, the value of the heat flux becomes its magnitude at the original level. This pattern of the parameter behavior is similar in the case of pressure distribution. The skin friction is at the same level in cases of separation between cylinder and plate. At $\Delta/r = 0$, its magnitude is negligible in the vicinity of the rear point.

The major effect of the plate location can be observed on the distributions of skin friction and heat flux along the plate surface (see Figs. 4 and 5). The skin friction is significantly less than predicted by the hypersonic-viscous-flow theory.[1] The heat flux distribution has maximum near the leading edge of the plate in the case of the plate location at $\Delta/r = 2$. In this case the width of the recirculation zone behind the cylinder is comparable with the distance between the cylinder and the leading edge of the plate.

Two Bluff Cylinders in-Tandem

Influence of Reynolds Number.

The flowfield around two identical irregular cylinders (with the generatrix $y/r = -0.5\cos(\pi x/2r)$ and located at $-3 \leqslant x/r \leqslant -1$ and $1 \leqslant x/r \leqslant 3$, correspondingly) was calculated at the Mach number $M_\infty = 5$ and the Reynolds number $Re_{\infty r} = 300$, 10^3, 10^4 and 10^5. It was assumed that $\gamma = 1.4$, and the body surface is isothermal at $T_w/T_\infty = 2$. The distance between the cylinders remains constant, $\Delta/r = 2$, in these study cases.

The distributions of flow parameters along the plane of symmetry in the wakes behind the cylinders and along their surfaces are shown in Figs. 6 and 7. The Reynolds number influences significantly the pressure and Mach number parameters. At $Re_{\infty r} \geqslant 10^4$, the zone between the cylinders is characterized by complex recirculation processes. The pressure distribution along the surface of the down-stream second cylinder changes significantly its pattern. The subsonic recirculation zone is developing behind this cylinder with increasing the Reynolds number.

The contours of constant values of local Mach number M are shown in Fig. 8 for four cases of the Reynolds numbers. The flow structure changes significantly with increasing the major similarity parameter of the Reynolds number. At $Re_{\infty r} \geqslant 10^4$, the zone between the cylinders becomes totally subsonic. As a result, the hot-gas area near the down-stream cylinder spreads far up-stream, up to the rear zone of the first cylinder. Behind the second cylinder, the wake area becomes narrow and it is filled with hot gas.

The normalized distributions of skin-friction coefficient and heat flux along the surfaces of cylinders are shown in Figs. 10 and 11. The developing recirculation zone between cylinders influences considerably these aerothermodynamic parameters on the rear surface of the first body and on the total surface of the down-stream cylinder. The extreme values of the skin-friction coefficient and heat flux do not coincide with each other at any parameter of the Reynolds number. It indicates that the "Reynolds analogy"[1] takes place only under the conditions of laminar non-separated flow near the up-stream surface of the first cylinder.

The calculating results of the drag coefficient are shown in Fig. 12. At small Reynolds numbers, $Re_{\infty r} \leqslant 10^3$, skin-friction component becomes predominant (this parameter of the first cylinder is larger by factor of 4.5 than the corresponding parameter of the down-stream body). At $Re_{\infty r} \geqslant 10^4$, the pressure component contributes prevalently into the drag coefficient of both cylinders, and the coefficient of the second cylinder changes non-monotonically with increasing the Reynolds number.

Influence of the Geometrical Factor, Δ/r.

The flow pattern is significantly sensitive to the major geometrical similarity parameter, Δ/r, where Δ is a distance between a rear point of the first cylinder and a front (stagnation) point of the second body in tandem. The influence of this parameter on the flow structure has been studied at the Mach number $M_\infty = 5$ and the Reynolds number $Re_{\infty r} = 10^4$.

The local Mach number and temperature contours are shown in Fig. 9 for four cases of a distance between bodies ($\Delta/r = 0.5$, 1, 2, and 3). At $\Delta/r \leqslant 1$, the ordinary wake structure behind the first cylinder is destroyed completely by the up-steaming flow from the second body. In all cases, the core of the wake becomes subsonic with recirculating.

The normalized distributions of skin-friction coefficient and heat flux along the cylinders surfaces are shown in Figs. 14 and 15 correspondingly. The skin-friction coefficient of the first cylinder becomes sensitive to the gasdynamic

processes in the recirculation zone between the bodies. This coefficient changes non-monotonically in the rear area of the cylinder with increasing a distance between the cylinders. At $\Delta/r \geq 2$, the distributions of the skin-friction coefficient and heat flux in this area have become unchangeable.

The main changes in distributions of the parameters C_f and q_w occur in the front area of the down-stream body (see Figs. 14b and 15b). The skin-friction coefficient increases monotonically with increasing the distance factor. The parameter of heat flux reaches its maximum value at Δ/r = 2, and after that it decreases with increasing parameter $\Delta/r \geq 3$. This fact indicates, that the Reynolds analogy is not applicable for the flow parameters in the front area of the second cylinder under the considered flow conditions.

The calculating results of the drag coefficient at constant Reynolds number, $Re_{\infty r} = 10^4$ are shown in Fig. 13. The pattern of drag-coefficient changes is absolutely different from the data in the case of incompressible viscous flow near cylinders in tandem, which was described by Blevins [10]. The discussed results indicate complex gasdynamic and thermodynamic processes in the compressible viscous flow about the bluff cylinders.

Torus Aerodynamics

Influence of the Geometrical Factor, H/R

The flow pattern over a torus is significantly sensitive to the major geometrical similarity parameter, H/R, where H is a distance between the axis of symmetry and the torus disk center, and R is a radius of a torus disk. The influence of this parameter on the flow structure has been studied for hypersonic flow of argon ($\gamma = 5/3$) at the Mach number $M_\infty = 10$, and the Knudsen number $Kn_{\infty R} = 0.1$. The wall temperature equals the stagnation temperature.

The Mach number contours are shown in Figs. 16 and 17 for two cases of the geometrical factor (H/R = 8 and 2). At $H/R = 8$, a conical shock wave can be observed near the torus. The interference of the shock waves takes in the form of the normal shock wave in the vicinity of the symmetry axis. At the intersection of the conical and normal shock waves, a new type of conical reflection wave has been found. The flow in this area is supersonic.

A local subsonic zone has been found behind the normal shock wave. The zone boundaries are restricted by supersonic conical flow behind the conical shock waves and the reflected waves. The size of the subsonic zone depends on the similarity parameters ($Kn_{\infty R}$, M_∞, γ, and H/R).

The shock-wave shape and the scale of the subsonic zone behind the shock wave are very sensitive to the geometrical parameter H/R. The reduction of the outer torus radius is a major factor of relocation of the local subsonic zone in upstream direction. At $H/R \leq 4$, the front-shock-wave shape becomes normal, and the subsonic area is restricted by the location of the shock wave and the torus throat (see Fig. 17). This effect plays a fundamental role in the redistribution of pressure and skin friction along the torus surface (see Figs. 18a and 18b, correspondingly; the angle θ changes from the torus rear point (θ = 0 deg) in the counter clockwise direction).

The dynamics of the subsonic zone is a major factor of relocation of the stagnation-points ring in the front area of the torus. This set of points can be identified by the radial velocity-component contours.[22] The location of the stagnation point is moving from the front area to the torus throat after reducing the outer torus radius. The similar effect can be observed in calculations of pressure and skin-friction coefficients (see Fig. 18).

Influence of the Knudsen number, Kn

The rarefaction factor, which can be characterized by the Knudsen number, plays important role in the flow structure[13] as well as in aerodynamics[1,4,8].

The flowfield about a torus has been calculated for hypersonic flow of argon at the Mach number $M_\infty = 10$, and the Knudsen numbers $Kn_{\infty R} = 0.0167$, 0.1, and 1.

The density contours at $H/R = 8$ and $Kn_{\infty R} = 0.0167$ and 1 are shown in Figs. 19a and 19b, correspondingly. Under continuum flow-regime conditions, the flow structure has the same features as were discussed above. In transitional-to-free-molecular flow regime, at $Kn_{\infty R} = 1$, the flow pattern is different. The reflection wave has different shape and characteristics, because of the rarefaction effects in the conic and normal shock waves.

At a small outer torus radius, H/R =2, the shin-friction coefficient distributions along the torus surface become sensitive to the rarefaction parameter $Kn_{\infty R}$ (see Figs. 20). The locations of the front stagnation points are not changed at different Knudsen numbers.

The calculating results of the total drag coefficient are shown in Fig. 21. At any outer-inner radii ratio, the drag coefficient increases with increasing the Knudsen number. The geometrical factor becomes insignificant on the drag at $H/R \geq 6$ under continuum flow regime conditions, and at $H/R \geq 4$ in free-molecule flow regime.

Conclusion

The flow parameters near a cylinder with no end contribution and a plate located in the wakes of a cylinder have been evaluated numerically for a wide range of geometrical parameters Δ/r. This parameter influences skin friction and heat flux distribution along the plate and cylinder surfaces.

The hypersonic viscous flow parameters near two irregular cylinders in-tandem have been evaluated numerically for a wide range of the Reynolds numbers. This parameter influences significantly the distributions of the pressure, skin friction and heat flux along the cylinders surfaces as well as the flow parameters in the wakes behind the bodies. At $Re_{\infty r} \geq 10^4$, the flow zone between the bluff cylinders has totally become subsonic with recirculating. This effect is responsible for significant change of skin-friction and heat-flux along the body surfaces. The drag coefficient of the down-stream cylinder changes non-

monotonously at high Reynolds numbers ($Re_{\infty r} \geq 10^4$).

It has been estimated that the maximum pressure parameter and the skin-friction coefficient on the second cylinder surface increases monotonically by 10% with increasing the distance between the bodies from $\Delta/r = 0.5$ to 3. At the same time, heat flux changes non-monotonically, reaching its maximum value at $\Delta/r = 2$. The Reynolds analogy between distributions of skin-friction and heat-flux characteristics does not take place in these cases.

The hypersonic rarefied-gas flow about a torus has been studied by the direct simulation Monte-Carlo technique. The flow pattern and shock-wave shapes are significantly different for small and large inner-outer-radii ratios. At the value of the ratio parameter equals 8, the conical shock waves interact in the vicinity of the symmetry axis, creating the normal shock wave (the Mach's disk). The reflected conical wave has different patterns of the interaction with the supersonic flow behind a torus in continuum and rarefied-gas flow regimes.

At the small ratio parameters, the front shock-wave shape becomes normal, the subsonic area is relocated in upstream direction. As a result of these significant changes, the front stagnation points relocate from the torus front zone towards the throat area. This phenomenon effects the drag, pressure and skin-friction distributions along the torus.

References

[1]Koppenwallner, G., "Fundamentals of Hypersonics: Aerodynamics and Heat Transfer," *Hypersonic Aerothermodynamics*, Lecture Series, No. 1984-01, DFVLR-AVA, Germany, February 1984, pp. 1-56.

[2]Oguchi, H., "The Sharp-Leading-Edge Problem in Hypersonic Flow," *Proceedings of the Second International Symposium on Rarefied Gas Dynamics*, Academic Press, New York, NY, 1961, pp. 501-524.

[3]Allegre, J., and C., Bisch, "Angle of Attack and Leading Edge Effects on the Flow about a Flat Plate at Mach Number 18," *AIAA Journal*, Vol. 6, No. 5, May 1968, pp. 848-852.

[4]Gusev, V. N., Erofeev, A. I., Klimova, T. V., Perepukhov, V. A., Riabov, V. V., and Tolstykh, A. I., "Theoretical and Experimental Investigations of Flow over Simple Shape Bodies by a Hypersonic Stream of Rarefied Gas," *Trudy TsAGI*, Issue 1855, 1977, pp. 3-43 (in Russian).

[5]Coudeville, H., Viviand, H., Raffin, M., and Brun, E. A., "An Experimental Study of Wakes of Cylinders at Mach 20 in Rarefied Gas Flow," *Proceedings of the Sixth International Symposium on Rarefied Gas Dynamics*, Vol. 1, Academic Press, New York, NY, 1969, pp. 881-894.

[6]Bashkin, V. A., Egorov, I. V., and Egorova, M. V., "Supersonic Viscous Perfect Gas Flow Past a Circular Cylinder," *Fluid Dynamics*, No. 6, Nov.-Dec. 1993, pp. 833-838.

[7]Bisch, C., "Drag Reduction of a Sharp Flat Plate in a Rarefied Hypersonic Flow," *Proceedings of the Tenth International Symposium on Rarefied Gas Dynamics*, Vol. 1, AIAA, Washington, D.C., 1976, pp. 361-377.

[8]Riabov, V. V., "Comparative Similarity Analysis of Hypersonic Rarefied Gas Flows near Simple-Shape Bodies," *AIAA Paper*, No. 97-2226, June 1997.

[9]Riabov, V. V., Yegorov, I. V., Ivanov, D. V., and Legner, H. H., "Numerical Study of Hypersonic Turbulent Flow About Segmented Projectiles," *AIAA Paper*, No. 98-2626, June 1998.

[10]Blevins, R. D., *Applied Fluid Dynamics Handbook*, Krieger Publishing Company, Malabar, Florida, 1992.

[11]Yegorov, I. V., Yegorova, M. V., Ivanov, D. V., and Riabov, V. V., "Numerical Study of Hypersonic Viscous Flow About Plates Located Behind a Cylinder," *AIAA Paper*, No. 97-2573, June 1997.

[12]Yegorov, I. V., Yegorova, M. V., and Riabov, V. V., "Analysis of Hypersonic Viscous Flow About Bluff Cylinders Placed One After Another," *AIAA Paper*, No. 98-0171, January 1998.

[13]Bird, G. A., *Molecular Gas Dynamics and the Direct Simulation of Gas Flows*, Oxford University Press, Oxford, 1994.

[14]Bird, G. A., "The DS2G Program User's Guide, Version 1.0," G.A.B. Consulting Pty, Killara, New South Wales, Australia, 1995.

[15]Yegorov, I., and Zaitsev, O., "Development of Efficient Algorithms for Computational Fluid Dynamic Problems," *Proceedings of the Fifth International Symposium on Computational Fluid Dynamics*, Sendai, 1993, Vol. III, pp. 393-400.

[16]Godunov, S. K., "Finite Difference Method for Numerical Computation of Discontinuous Solutions of the Equations of Fluid Dynamics," *Matematicheskii Sbornik*, Vol.47, 1959, pp. 271-306 (in Russian).

[17]Roe, P. L., "Approximate Riemann Solvers, Parameter Vectors, and Difference Scheme," *Journal of Computational Physics*, Vol. 43, 1981, pp. 357-372.

[18]Kolgan, V. P., "Application of the Principle of Minimum Value of Derivatives to the Construction of Finite-Difference Schemes for Calculating Discontinuous Solutions of Gas Dynamics," *Uchenye Zapiski TsAGI*, Vol. 3, No. 6, 1972, pp. 68-77 (in Russian).

[19]Yegorov, I. V., and Ivanov, D. V., "Application of the Complete Implicit Monotonized Finite-Differential Schemes in Modeling Internal Plane Flows," *Journal of Computational Mathematics and Mathematical Physics*, Vol. 36, No. 12, 1996, pp. 91-107.

[20]Bashkin, V. A., Yegorov, I. V., and Ivanov, D. V., "Application of Newton's Method to Calculation of Supersonic Internal Separation Flows," *Journal of Applied Mechanics and Technical Physics*, Vol.37, No.1, 1997.

[21]Lipton, R. J., Rose, D. J., and Tarjan, R. E., "Generalized Nested Dissection," *SIAM Journal of Numerical Analysis*, Vol. 16, 1979, pp. 346-351.

[22]Riabov, V. V., "Numerical Study of Hypersonic Rarefied-Gas Flow About a Torus," *AIAA Paper*, No. 98-0778, January 1998.

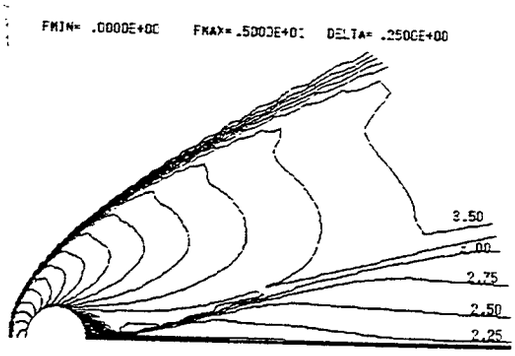

FIGURE 1 - Mach Number Contours above a Cylinder and Plate at $Re_\infty = 10^5$, $M_\infty = 5$, and $\Delta/r = 2$.

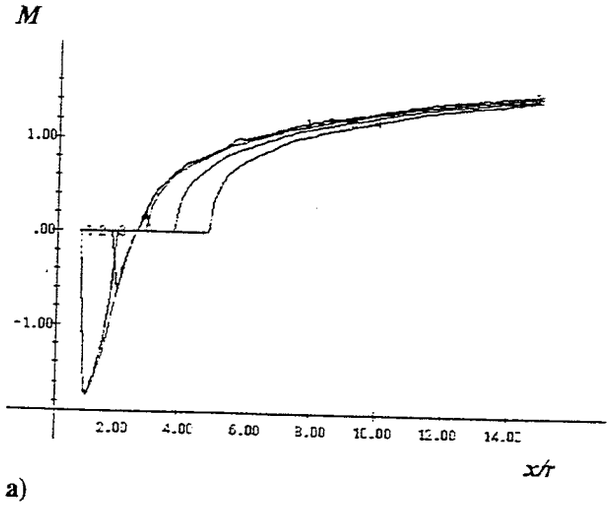

a)

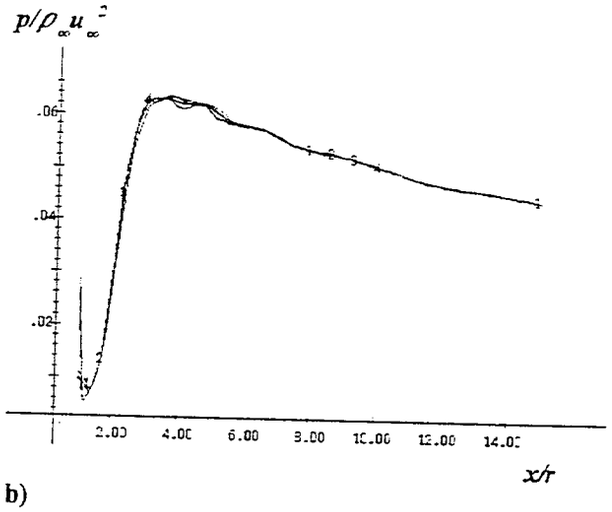

b)

FIGURE 2 - Mach Number and Pressure Along the Plane of Symmetry in the Wakes behind a Cylinder at $Re_\infty = 10^5$. Curve 1 - Cylinder without a Plate; 2 - Cylinder and Plate, $\Delta/r = 0$; 3 - $\Delta/r = 1$; 4 - $\Delta/r = 2$.

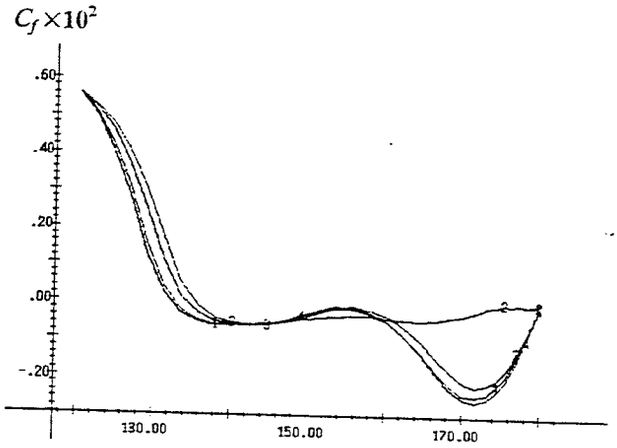

a)

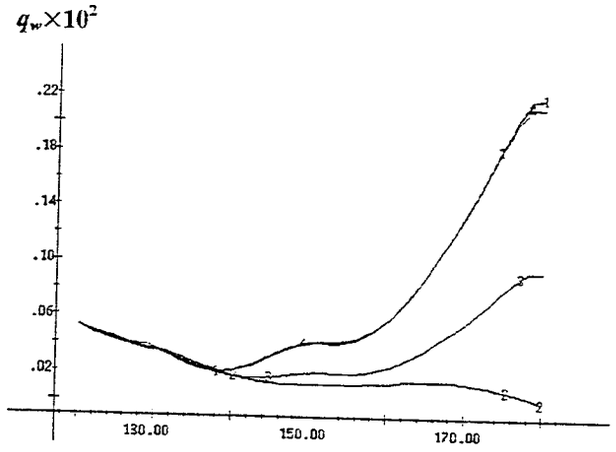

b)

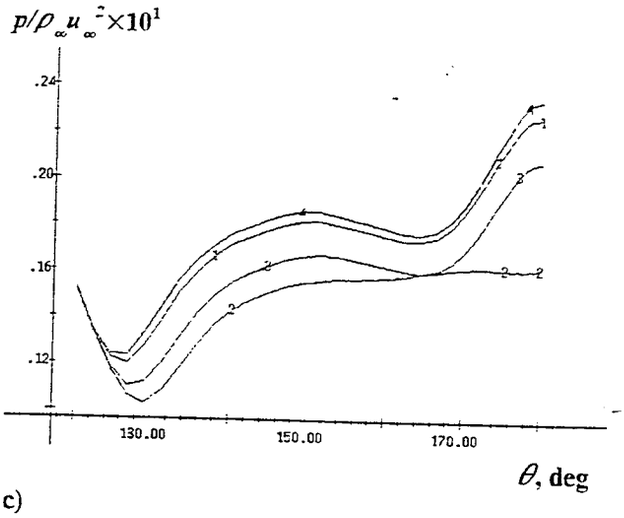

c)

FIGURE 3 - Skin-Friction Coefficient, Heat Flux, and Pressure Along the Rear Surface of a Cylinder at $Re_\infty = 10^4$. Curve 1 - Cylinder without a Plate; 2 - Cylinder and Plate, $\Delta/r = 0$; 3 - $\Delta/r = 1$; 4 - $\Delta/r = 2$.

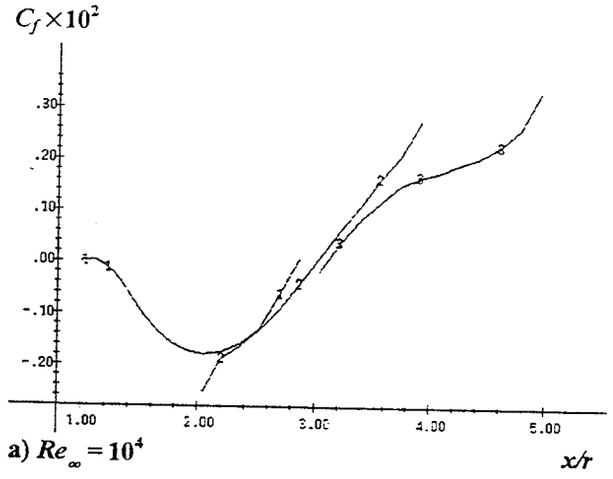

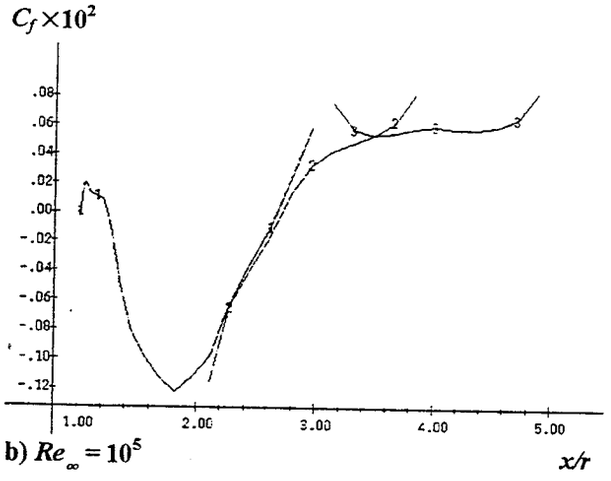

FIGURE 4 - Skin-Friction Coefficient Along the Plate Surface at $M_\infty = 5$. Curve 1 - Cylinder and Plate, $\Delta/r = 0$; Curve 2 - $\Delta/r = 1$; Curve 3 - $\Delta/r = 2$.

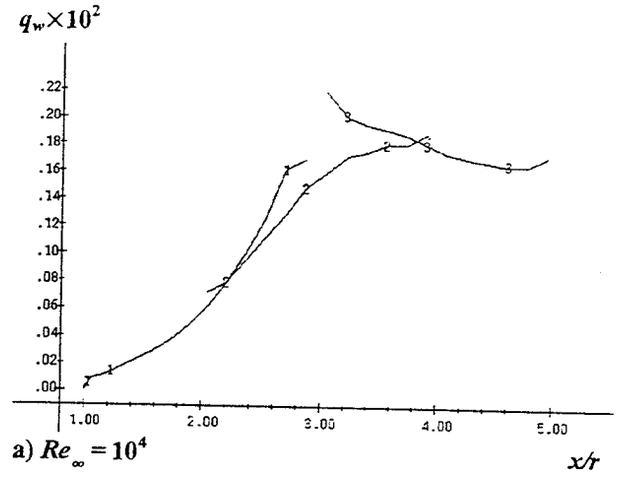

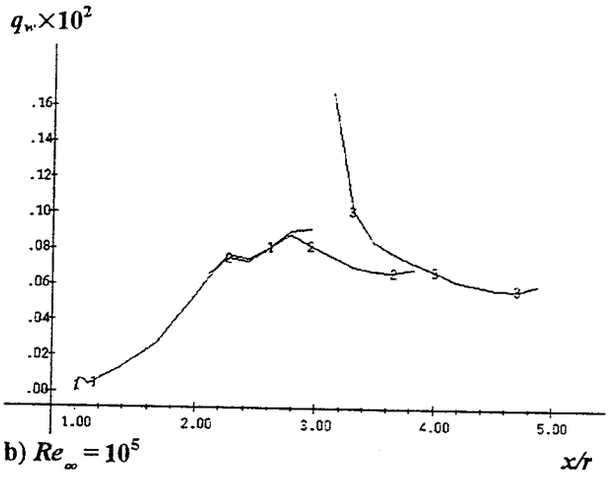

FIGURE 5 - Heat Flux Along the Plate Surface at $M_\infty = 5$. Curve 1 - Cylinder and Plate, $\Delta/r = 0$; Curve 2 - $\Delta/r = 1$; Curve 3 - $\Delta/r = 2$.

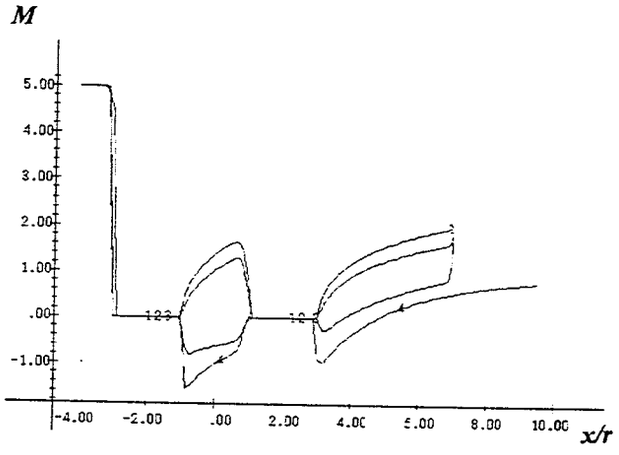

FIGURE 6 - Mach Number Along the Symmetry Plane in the Wakes Behind Cylinders at $\Delta/r = 2$, $M_\infty = 5$. Curve 1 - $Re_\infty = 300$; 2 - $Re_\infty = 1000$; 3 - $Re_\infty = 10^4$; 4 - $Re_\infty = 10^5$.

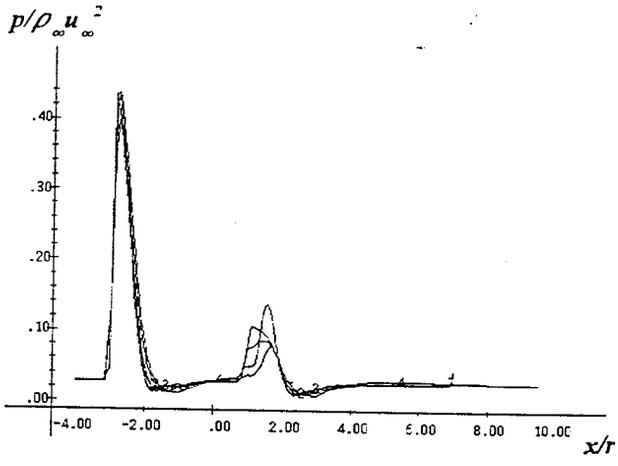

FIGURE 7 - Pressure Along the Symmetry Plane in the Wakes Behind Cylinders at $\Delta/r = 2$, $M_\infty = 5$. Curve 1 - $Re_\infty = 300$; 2 - $Re_\infty = 1000$; 3 - $Re_\infty = 10^4$; 4 - $Re_\infty = 10^5$.

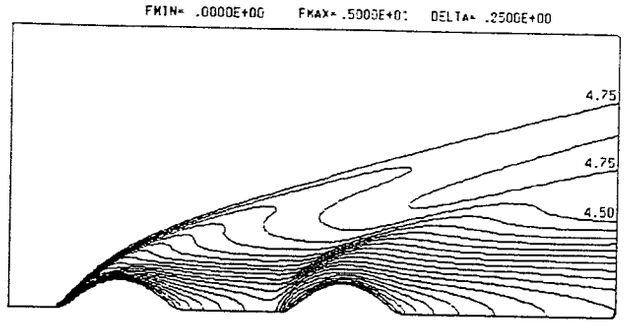

a) $Re_\infty = 300$

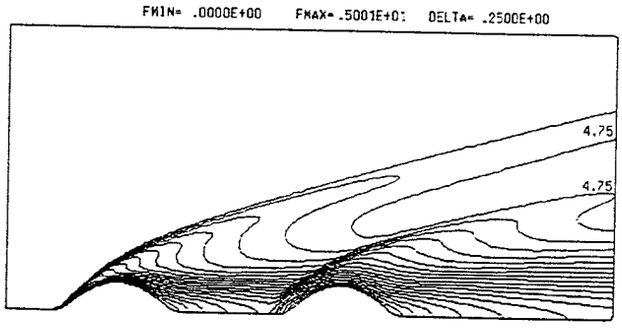

b) $Re_\infty = 1000$

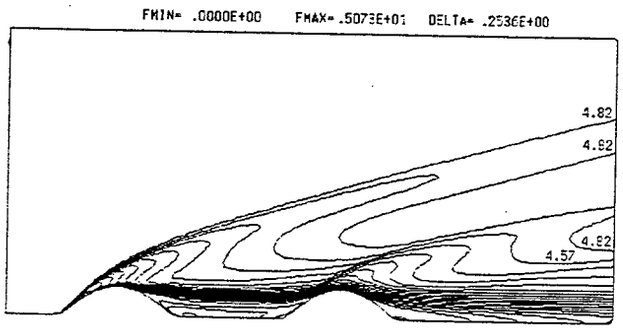

c) $Re_\infty = 10^4$

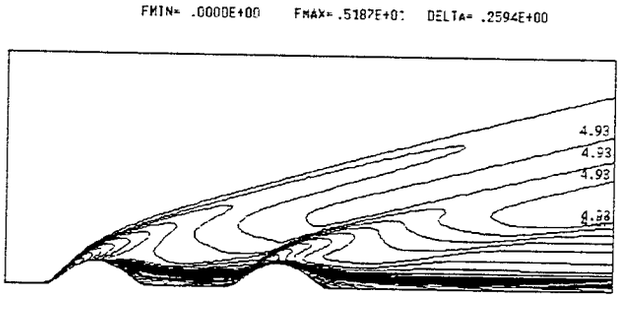

d) $Re_\infty = 10^5$

FIGURE 8 - Mach Number Contours at $\Delta/r = 2$ and $M_\infty = 5$.

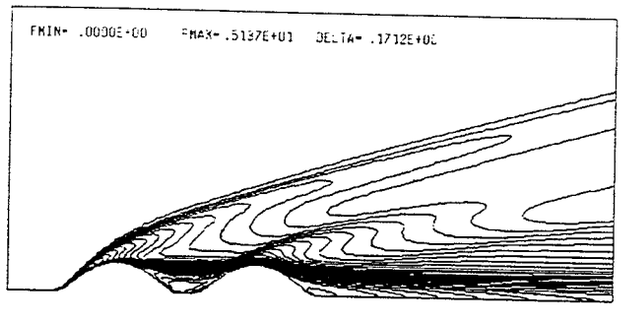

a) $\Delta/r = 0.5$

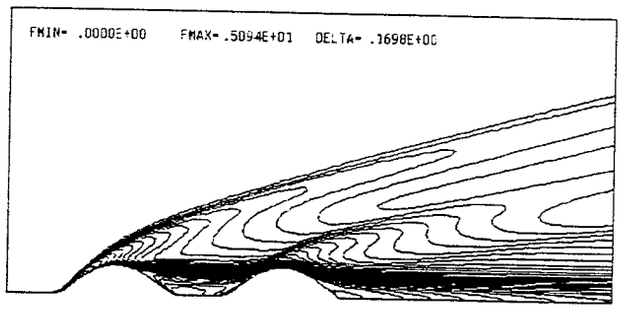

b) $\Delta/r = 1$

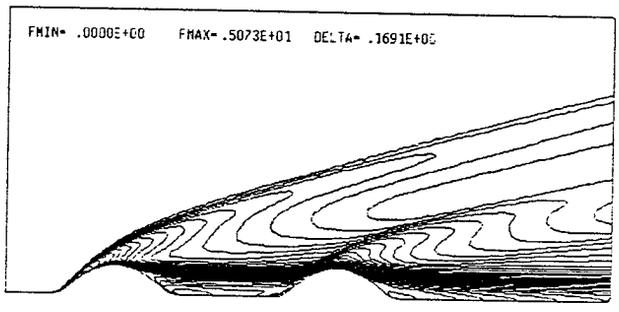

c) $\Delta/r = 2$

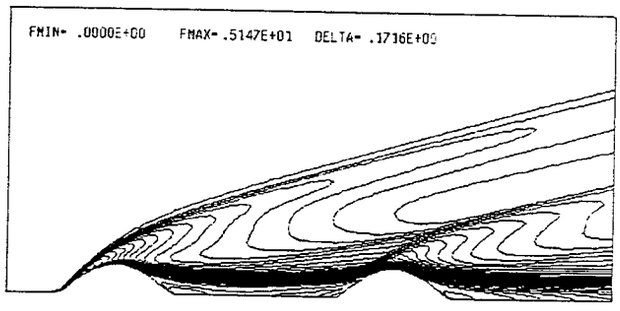

d) $\Delta/r = 3$

FIGURE 9 - Mach Number Contours at $Re_\infty = 10^4$.

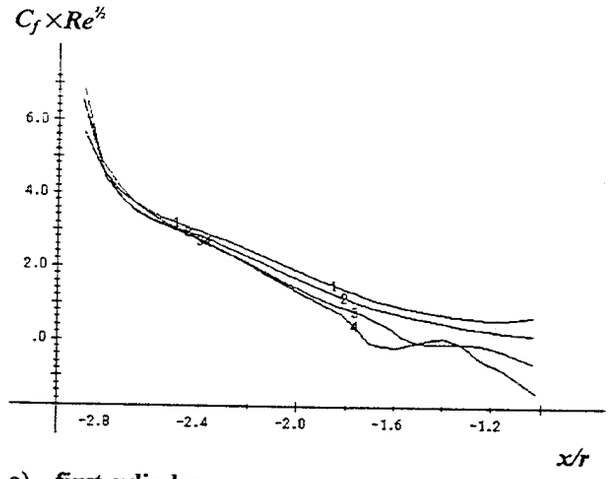

a) first cylinder

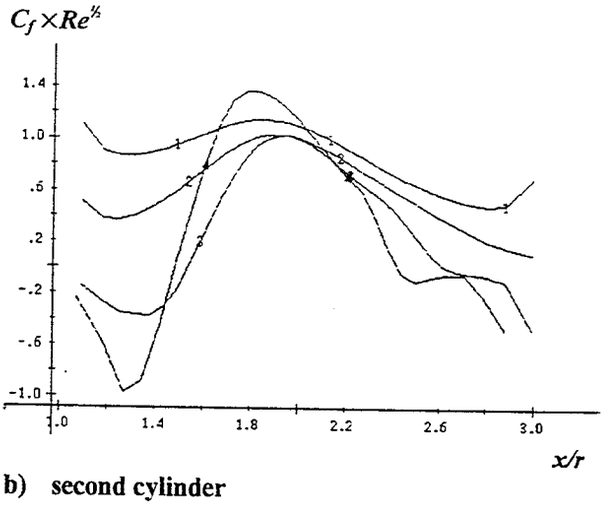

b) second cylinder

FIGURE 10 - Skin-Friction Coefficient Along the Surfaces of Cylinders at $\Delta/r = 2$. Curve 1 - $Re_\infty = 300$; 2 - $Re_\infty = 1000$; 3 - $Re_\infty = 10^4$; 4 - $Re_\infty = 10^5$.

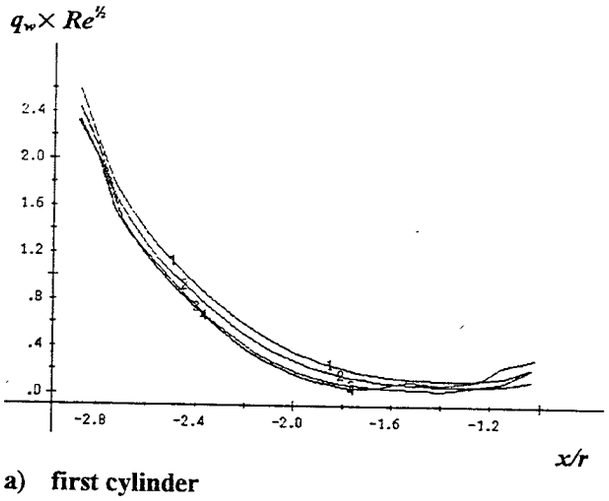

a) first cylinder

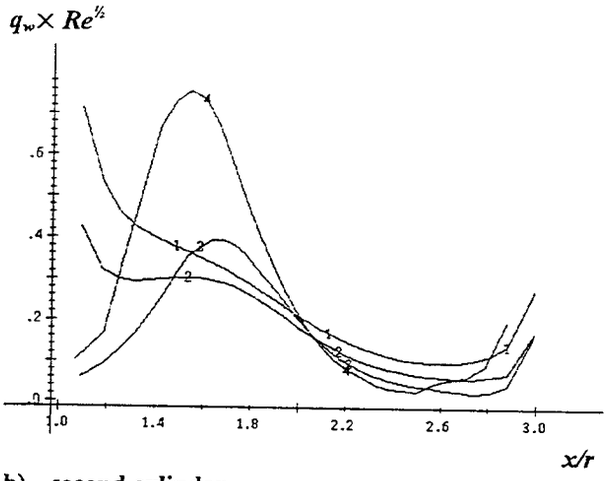

b) second cylinder

FIGURE 11 - Heat Flux Along the Surfaces of Cylinders at $\Delta/r = 2$. Curve 1 - $Re_\infty = 300$; 2 - $Re_\infty = 1000$; 3 - $Re_\infty = 10^4$; 4 - $Re_\infty = 10^5$.

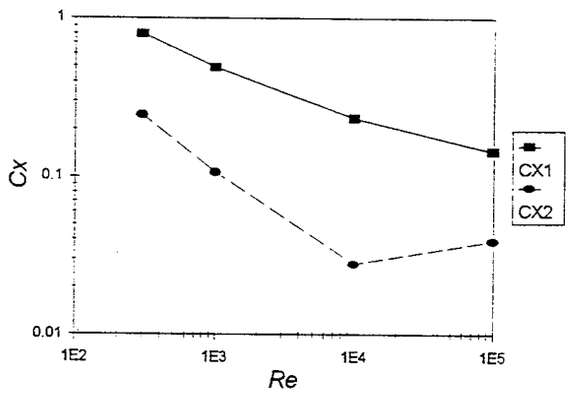

FIGURE 12 - The Drag Coefficient vs the Reynolds Number Re_∞ at $\Delta/r = 2$ and $M_\infty = 5$. Indexes 1 and 2 correspond to the first and second cylinders.

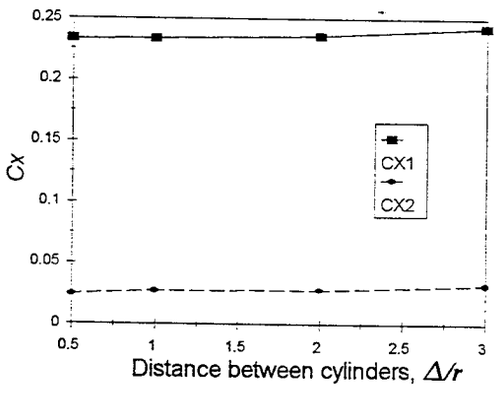

FIGURE 13 - The Drag Coefficient vs the Distance between Bluff Cylinders Δ at Reynolds Number $Re_\infty = 10^4$ and $M_\infty = 5$. Indexes 1 and 2 correspond to the first and second cylinders.

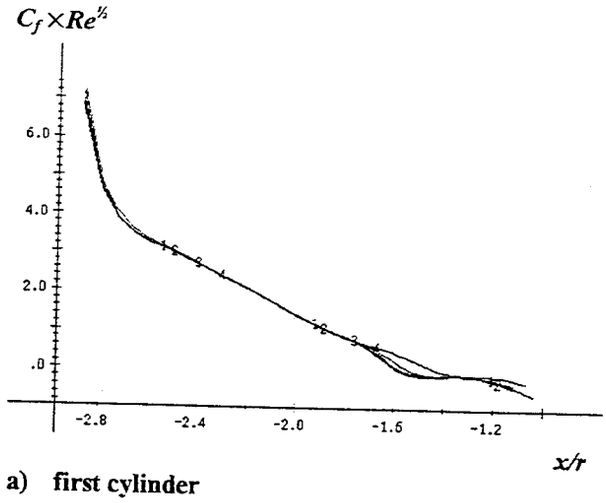

a) first cylinder

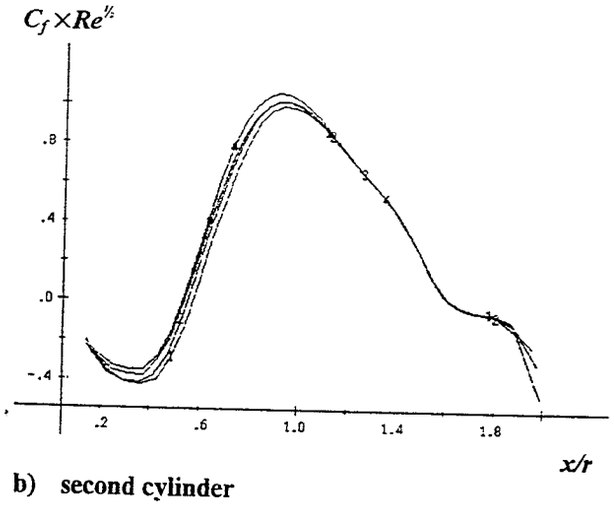

b) second cylinder

FIGURE 14 - Skin-Friction Coefficient Along the Surfaces of Cylinders at $Re_\infty = 10^4$. Curve 1 - Δ/r = 0.5; 2 - Δ/r = 1; 3 - Δ/r = 2; 4 - Δ/r = 3.

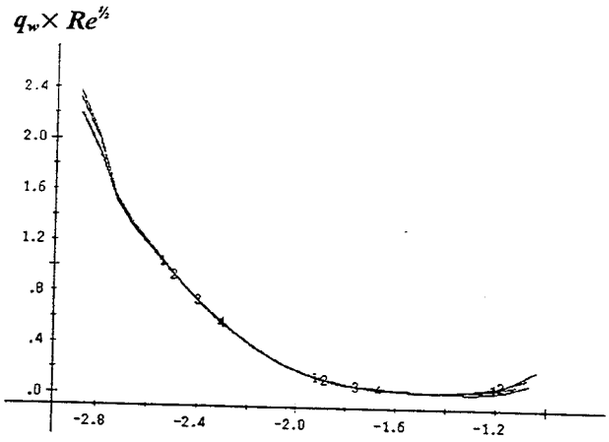

a) first cylinder

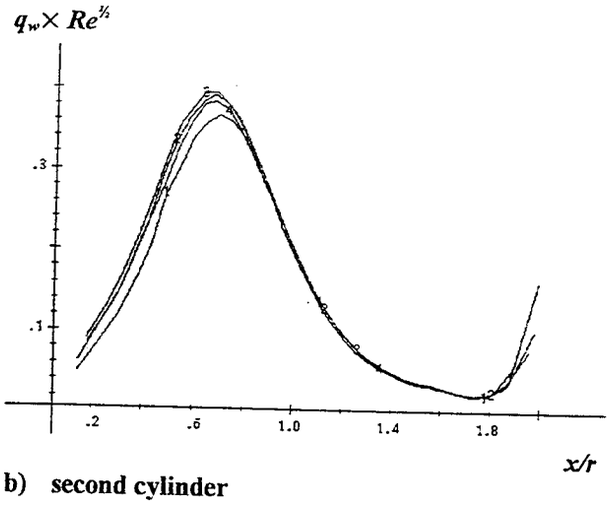

b) second cylinder

FIGURE 15 - Heat Flux Along the Surfaces of Cylinders at $Re_\infty = 10^4$. Curve 1 - Δ/r = 0.5; 2 - Δ/r = 1; 3 - Δ/r = 2; 4 - Δ/r = 3.

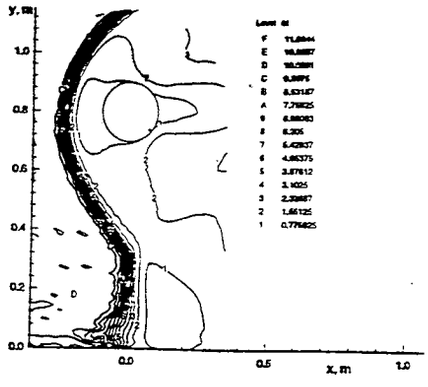

FIGURE 16 - Mach Number Contours in Argon Flow About a Torus at $Kn_{\infty R}$ = 0.1, H/R = 8, and M_∞ = 10.

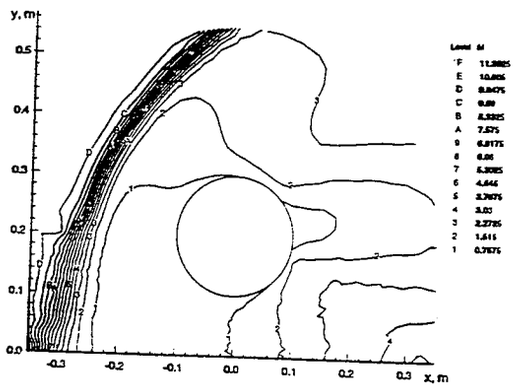

FIGURE 17 - Mach Number Contours in Argon Flow About a Torus at $Kn_{\infty R}$ = 0.1, H/R = 2, and M_∞ = 10.

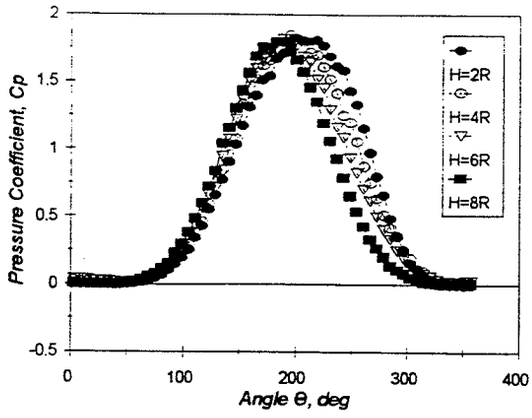

a) **Pressure Distribution**

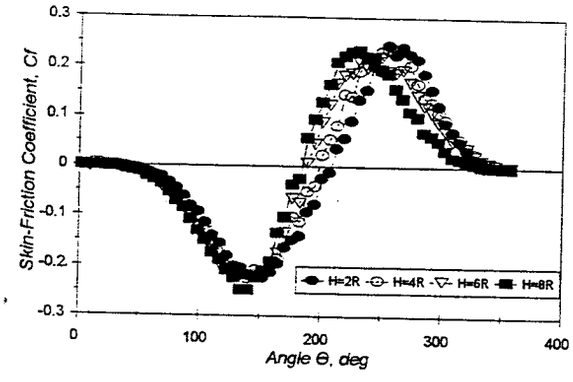

b) **Shear-Stress Distribution**

FIGURE 18 - Pressure and Skin-Friction Coefficients Along the Torus Surface at $Kn_{\infty R} = 0.1$ and $M_\infty = 10$.

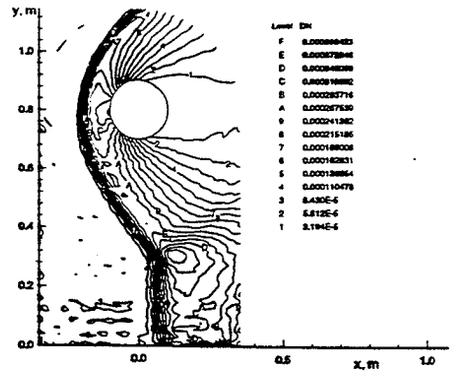

a) $Kn_{\infty R} = 0.0167$

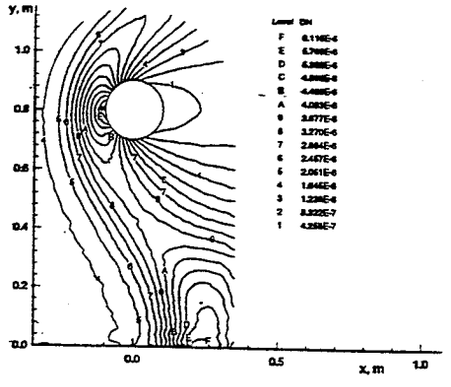

b) $Kn_{\infty R} = 1$

FIGURE 19 - Density Contours in Argon Flow About a Torus at $M_\infty = 10$ and $H/R = 8$.

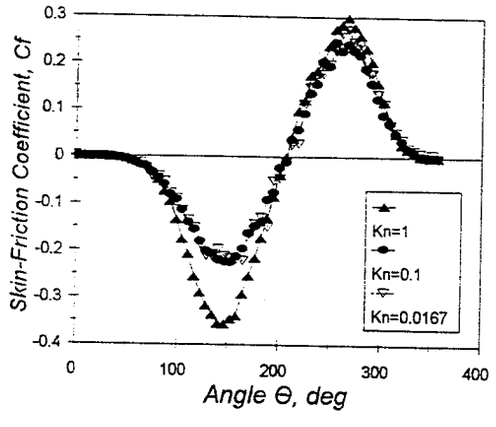

FIGURE 20 - The Skin-Friction Coefficient Along the Torus Surface at $H/R = 2$ and $M_\infty = 10$.

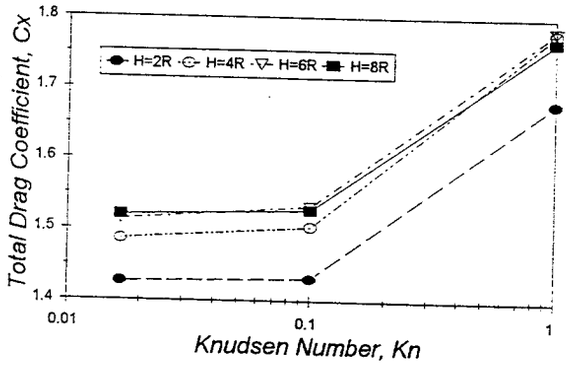

FIGURE 21 - Total Drag Coefficient of the Torus vs the Knudsen Number, $Kn_{\infty R}$ in Argon at $M_\infty = 10$.